Relationship between neighbor number and vibrational spectra in disordered colloidal clusters with attractive interactions

Peter J. Yunker,[1] Zexin Zhang,[2,3] Matthew Gratale,[1] Ke Chen,[4] and A. G. Yodh[1]
[1]*Department of Physics and Astronomy, University of Pennsylvania, Philadelphia Pennsylvania 19104, USA*
[2]*Center for Soft Condensed Matter Physics and Interdisciplinary Research, Soochow University, Suzhou 215006, China*
[3]*Complex Assemblies of Soft Matter, CNRS-Rhodia-UPenn UMI 3254, Bristol, Pennsylvania 19007, USA*
[4]*Beijing National Laboratory for Condensed Matter Physics and Key Laboratory of Soft Matter Physics, Institute of Physics, Chinese Academy of Sciences, Beijing 100190, China*

(Received 17 October 2012; accepted 18 December 2012; published online 11 January 2013)

We study connections between vibrational spectra and average nearest neighbor number in disordered clusters of colloidal particles with attractive interactions. Measurements of displacement covariances between particles in each cluster permit calculation of the stiffness matrix, which contains effective spring constants linking pairs of particles. From the cluster stiffness matrix, we derive vibrational properties of corresponding "shadow" glassy clusters, with the same geometric configuration and interactions as the "source" cluster but without damping. Here, we investigate the stiffness matrix to elucidate the origin of the correlations between the median frequency of cluster vibrational modes and average number of nearest neighbors in the cluster. We find that the mean confining stiffness of particles in a cluster, i.e., the ensemble-averaged sum of nearest neighbor spring constants, correlates strongly with average nearest neighbor number, and even more strongly with median frequency. Further, we find that the average oscillation frequency of an individual particle is set by the total stiffness of its nearest neighbor bonds; this average frequency increases as the square root of the nearest neighbor bond stiffness, in a manner similar to the simple harmonic oscillator. © *2013 American Institute of Physics*. [http://dx.doi.org/10.1063/1.4774076]

I. INTRODUCTION

Colloidal particles that interact via strong short-range attractive potentials form disordered clusters,[1,2] and these clusters often have large *local* packing fractions and particle configurations similar to common "space-filling" colloidal glasses. Recent experiments[3] have suggested that the vibrational properties of small clusters of colloidal particles with attractive interactions are similar to the vibrational properties of jammed glasses.[4,5] Specifically, the median frequency of the cluster vibrational spectrum, ω_{Med}, was found to correlate strongly with the average number of neighbors, $\overline{NN}$, in the cluster. This behavior resembles that in simulations of mechanically stable athermal jammed packings, wherein the so-called Boson peak frequency scales linearly with the average number of contacts between particles.[5] Thus, further exploration of the strong correlation between $\overline{NN}$ and ω_{Med} holds potential to distinguish properties universal to disordered systems (e.g., Refs. 3 and 5) from properties that are system specific (e.g., Ref. 6).

In this contribution we experimentally investigate the vibrational properties of disordered clusters of colloidal particles with attractive interactions. Disordered clusters are formed in water-lutidine suspensions wherein wetting effects induce fluid mediated attraction between micron-sized polystyrene particles.[6–9] Each cluster is characterized by the number of particles it contains (N) and its average number of nearest neighbors ($\overline{NN}$). Displacement covariance matrix techniques employed in recent papers[10–13] are then used to determine phonon spectra of each attractive glassy cluster. Specifically, video microscopy is employed to measure displacement covariances between each particle pair in each cluster. Using this information, we calculate the cluster stiffness matrix, K_{ij}, which contains the effective spring constants that link each pair of particles i and j. From the stiffness matrix, we derive the phonon density of states of corresponding "shadow" attractive glass clusters with the same geometric configuration and interactions as the "source" experimental colloidal system, but absent damping.[11] While numerical simulations can also access the vibrational density of states of disordered systems (e.g., Ref. 5), the results presented here are from real clusters that self-assembled via complex interactions or were assembled with laser tweezers. Thus, these results are relevant for real systems that can easily be made in the lab, as opposed to idealized model systems.

Previous work has demonstrated that the median cluster vibrational frequency, ω_{Med}, depends strongly on the average number of nearest neighbors, $\overline{NN}$, but weakly on the number of particles, N, in the cluster, and weakly on other structural parameters of the cluster.[3] The present experiments reveal that ω_{Med} has an even stronger correlation with the mean stiffness felt by individual particles than with $\overline{NN}$, i.e., the mean of the diagonal elements of the stiffness matrix, $\overline{K}_{ii}$ compared to $\overline{NN}$. $\overline{K}_{ii}$, in turn, is shown to be correlated with $\overline{NN}$, among other factors. This experimental observation is further supported by a simple theoretical argument. In addition, we find that the average oscillation frequency of any given particle in the cluster increases as the square root of its total nearest

neighbor bond stiffness, similar to the behavior of a simple harmonic oscillator. Thus, while global spectral properties are controlled, in large part, by network connectivity, local vibrational properties are controlled by local stiffness. Finally, the work provides microscopic evidence that spectroscopic observations can be used to probe structural coordination properties of disordered media.

II. BACKGROUND

A. Experimental system

The experiments employ bidisperse suspensions of micron-sized polystyrene particles (Invitrogen), with diameters of $d_S = 1.5\ \mu$m and $d_L = 1.9\ \mu$m, and number ratio of 1:2, respectively. Binary mixtures of particles were used to minimize crystallization. Particles were suspended in a mixture of water and 2, 6-lutidine (WL) near its critical composition, i.e., a lutidine mass fraction of 0.28. Colloidal particles in this near-critical WL binary mixture experience temperature dependent fluid-mediated repulsive or attractive interactions.[7,8] Particles are well dispersed at $T = 300.15$ K, but at $T = 306.45$ K they aggregate and form clusters, because lutidine preferentially wets the polystyrene particles.

A plethora of different disordered particle clusters are created by first suspending particles deep in the repulsive regime (300.15 K), and then rapidly increasing the sample temperature (to 306.5) *in situ*.[3] Sample temperature control was accomplished using an objective heater (Bioptechs) connected to the microscope oil immersion objective.[14–16] Particles are confined between two glass coverslips (Fisher) with a spacing of $\sim 1.1 \pm 0.05 d_L$; the sample is therefore a quasi-2D system. The glass cell was treated with hexamethyldisilazane (HMDS), so the particle-wall interaction potential is repulsive at relevant temperatures.[9] The global area fraction is $\sim$0.2.

Disordered clusters of various sizes and shapes self-assemble. Other clusters are created with aid of laser tweezers,[17] either by grabbing particles and adding them to existing clusters, or by dragging an optical trap across a cluster and forcing rearrangements. Samples equilibrated for about six hours before measurements began. Video data were collected at a rate of 10 frames per second.

The number of particles, N, is only weakly correlated with $\overline{NN}$ (Fig. 1). For linear clusters ($\overline{NN} < 2$), N and $\overline{NN}$ have a strong correlation; for more compact clusters ($\overline{NN} \geq 2$), N and $\overline{NN}$ have a very weak correlation.

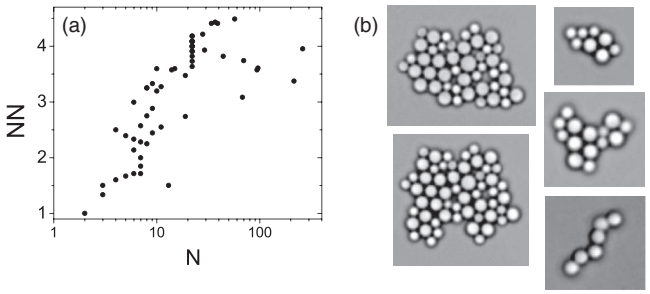

FIG. 1. (a) Plot summarizing the number of particles, N, and average number of nearest neighbors, $\overline{NN}$, in every cluster studied. (b) Experiment snapshots of five different clusters.

Note, Fig. 1(a) is plotted on a linear-log plot. Thus, while it appears N and $\overline{NN}$ may be strongly correlated for $N < 20$, this is not the case (for $N < 20$, $R^2 = 0.37$).

B. Theoretical analysis

The vibrational properties of each cluster are extracted by measuring displacement correlations of the particles within each cluster. Specifically, we define $u(t)$ as the $2N$-component vector of the displacements of all particles from their average positions $(\overline{x}, \overline{y})$, and we extract the time-averaged displacement correlation matrix (covariance matrix), $C_{ij} = \langle u_i u_j \rangle_t$, from experiment, where $i, j = 1, \ldots, 2N$ run over all particle and positional coordinates, and the average runs over time. Note, the calculation of C_{ij} depends only on particle displacements. In the harmonic approximation, the correlation matrix is directly related to the cluster stiffness matrix, defined as the matrix of second derivatives of the effective pair interaction potential with respect to particle position displacements. In particular, $(C^{-1})_{ij} k_B T = K_{ij}$, where K_{ij} is the stiffness matrix. Experiments that measure C therefore permit us to construct and derive properties of a "shadow" glassy cluster that has the same static properties as our colloidal system (e.g., same correlation matrix, same stiffness matrix, etc.).[11–13] Following Ref. 18, we expect undamped particles, that repel at very short-range and attract on longer length scales, due to fluid mediated effects, to give rise to solid-like vibrational behavior on time scales long compared to particle collision times, but short compared to the time between particle rearrangement events.[10,13]

The stiffness matrix is directly related to the dynamical matrix characterizing system vibrations, $D_{ij} = \frac{K_{ij}}{m_{ij}}$, where $m_{ij} = \sqrt{m_i m_j}$ and m_i is the mass of particle i. The eigenvectors of the dynamical matrix correspond to particle displacement amplitudes associated with the various phonon modes, and the eigenvalues of the dynamical matrix are the frequencies/energies of the corresponding modes. Data were collected for 10 000 s so that the number of degrees of freedom, $8 \leq 2N \leq 500$, is small compared to the number of time frames ($>10 \times 2N$). Additionally, we find K_{ij} is far above the noise only for adjacent particles, as expected.

C. Finite-sampling correction

To correct for finite-time effects, we extrapolate to "infinite time" and derive "true" frequencies. To this end, we use the relationship $1/\omega(N_{frames}) = 1/\omega(\text{inf}) + m2N/N_{frames}$, where N_{frames} is the number of images collected, $2N$ is the number of degrees of freedom in the sample, and m is a multiplicative constant (Fig. 2).[19] This correction was found to have little effect on ω_{Med}; i.e., the coefficient of determination, $R^2 = 0.85$, was unchanged when comparing corrected and uncorrected frequencies.

As a side note, the correlation does not depend on particle size. We plotted the median frequency versus the average number of neighbors for large particles and the average number of neighbors for small particles. The correlation persists, but is weaker. The best linear fits for $NN > 2$ yield $R^2 = 0.80$ and $R^2 = 0.67$ for small and large particles,

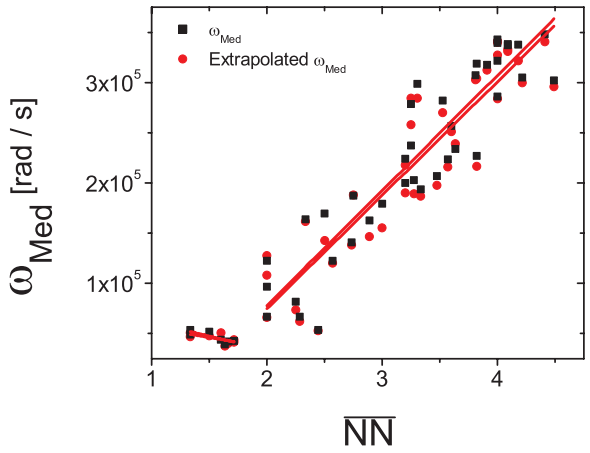

FIG. 2. The median frequency, ω_{Med} (black squares), and the infinite-time-extrapolated median frequency (red circles), are plotted versus the average number of nearest neighbors, $\overline{NN}$.

respectively. Thus, the correlation is at its strongest when both large and small particles are considered.

III. RESULTS

A. Effect of $\overline{K_{ii}}$ on ω_{Med}

Interestingly, that data reveal that a strong relationship exists between ω_{Med} and $\overline{NN}$, despite the fact that $\overline{NN}$ does not directly enter into any calculation of ω_{Med} (Fig. 2). Thus, information about $\overline{NN}$ must be implicit in K_{ij}. In fact, the average of the diagonal elements in the stiffness matrix, $\overline{K}_{ii}$, has a strong correlation with $\overline{NN}$ too (Fig. 3). This effect might be expected, since the diagonal elements of the stiffness matrix typically balance out the springs of neighbors pushing against the selected particle i, i.e., $\sum_{j\neq i} K_{ij} \approx -K_{ii}$. Here, each spring represents the strength of the harmonic interaction between particle i and particle j, and K_{ii} is essentially the curvature of the harmonic potential well that confines particle i. Since the sum is dominated by the nearest neighbor springs (i.e., non-nearest neighbor spring constants are approximately zero), K_{ii} depends strongly on the neighbor number of particle i. Thus, as $\overline{NN}$ increases, $\overline{K_{ii}}$ tends to increase as well, i.e., more neighbors lead to stronger confinement. $\overline{K_{ii}}$ can also increase

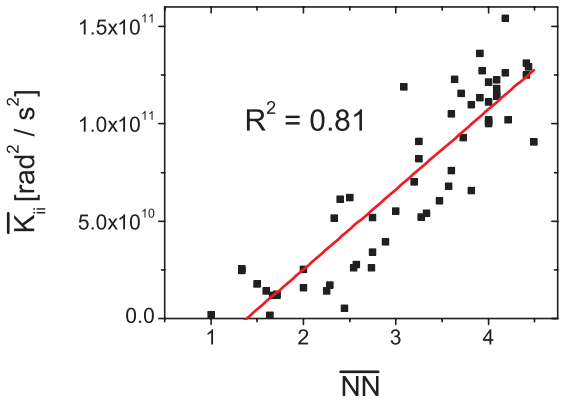

FIG. 3. The mean of the diagonal value of the stiffness matrix, i.e., $\overline{K}_{ii}$, plotted versus the average number of nearest neighbors in the cluster, $\overline{NN}$.

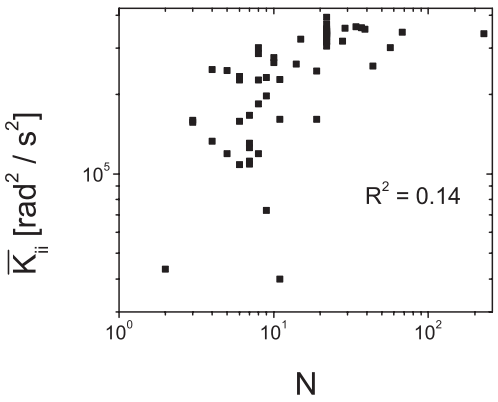

FIG. 4. The mean of the diagonal value of the stiffness matrix, i.e., $\overline{K}_{ii}$, plotted versus the total number of particles in the cluster, N.

(or decrease) without changing average $\overline{NN}$, for example via changes of the interparticle separation between neighboring particles.

Conversely, $\overline{K_{ii}}$ has relatively little correlation with the total number of particles in a cluster, N (see Fig. 4). This weak correlation ($R^2 = 0.14$) is expected, since non-nearest-neighbor spring constants are ~0, and the sum $\sum_{j\neq i} K_{ij}$ only depends strongly on $\overline{NN}$.

We next investigated the relationship between $\overline{K}_{ii}$ and ω_{Med}. The correlation between these two parameters is very strong; the coefficient of determination is $R^2 = 0.92$ (Fig. 5 inset). In fact, this correlation is even stronger than the one observed between ω_{Med} and $\overline{NN}$ (Fig. 2). Finally, we investigated the correlation between $\sqrt{\overline{K}_{ii}}$ and ω_{Med} (Fig. 5), since $K_{ij}e_i = \omega^2 e_i$, where e_i is the polarization of mode i. The correlation between these two parameters is also very strong, with a coefficient of determination $R^2 = 0.93$, and the best linear fit of $\sqrt{\overline{K}_{ii}}$ and ω_{Med} gives $\omega_{Med} \propto 1.09(4)\sqrt{\overline{K}_{ii}}$. The latter observation implies that $\sqrt{\overline{K}_{ii}}$ and ω_{Med} increase with a nearly 1-to-1 ratio; note, however, the accessible dynamic range is not large enough for a power-law fit to unambiguously distinguish between $\omega_{Med} \propto \overline{K}_{ii}$ and $\omega_{Med} \propto \sqrt{\overline{K}_{ii}}$, even though a very strong correlation exists.

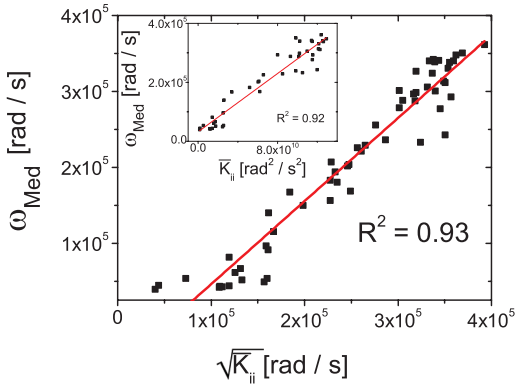

FIG. 5. The median vibrational frequency of cluster mode spectra versus the square root of the mean of the diagonal value of the cluster stiffness matrix, i.e., $\sqrt{\overline{K}_{ii}}$. Black squares and red circles represent clusters with $\overline{NN} \geq 2$ and $\overline{NN} < 2$, respectively. Inset: The median vibrational frequency of cluster mode spectra versus the mean diagonal value of the cluster stiffness matrix, i.e., $\overline{K}_{ii}$.

The strong correlation between $\sqrt{\overline{K_{ii}}}$ and ω_{Med} is self-consistent with the fact that ω_{Med} is largely independent of N; $\overline{K_{ii}}$ is strongly correlated with $\overline{NN}$ (Fig. 3), but only weakly correlated with N (Fig. 4). Physically, increasing the number of nearest neighbors increases the number of bonds in a particle's confining "cage," and is a factor that strongly affects K_{ii}. However, the average number of neighbors in a cluster is only weakly correlated with the number of particles in a cluster, N (Fig. 1). A simple theoretical derivation of the correlation between $\sqrt{\overline{K_{ii}}}$ and ω_{Med} is provided in the Appendix. In essence, K_{ij} can formally be written as the sum of a matrix, A_{ij}, and the identity matrix multiplied by $\overline{K_{ii}}$. The median frequency of K_{ij} is then the median frequency of A_{ij} plus $\overline{K_{ii}}$; thus, $\omega_{Med} \propto \overline{K_{ii}}$.

As a side note, the correlation between ω_{Med} and $\overline{K_{ii}}$ does not depend on particle size. We plotted the median frequency versus the average number of neighbors for large particles and the average number of neighbors for small particles. The correlation persists, but is weaker. The best linear fits for $NN > 2$ yield $R^2 = 0.60$ and $R^2 = 0.82$ for small and large particles, respectively. Thus, the correlation is at its strongest when both large and small particles are considered.

Finally, we note that the previously observed[3] relationship between ω_{Med} and NN had two regimes, suggesting a clear distinction between the effects of locally rigid structures ($\overline{NN} > 2$) and purely floppy structures ($\overline{NN} < 2$). In the present experiment, however, the observed relationship between $\overline{K_{ii}}$ and ω_{Med}, does not clearly separate into two regimes and thus does not readily distinguish between the effects of these qualitatively different structures. This scenario arises partially due to the limitations of calculating a meaningful median vibrational frequency. For clusters with $\overline{NN} < 2$, more than half of the modes are floppy. These modes have small frequencies, independent of $\overline{K_{ii}}$, which are nearly zero. Thus, the median frequency for these clusters does not depend on $\overline{K_{ii}}$.

B. Vibrational properties of individual particles

To explore local vibrational properties around each particle, we calculate the polarization vector-weighted frequency $\langle\omega_{i\alpha}\rangle = \sum_{j=1..2N} \omega(j) * e(j)_i^2 / \sum_{j=1..2N} e(j)_{i\alpha}^2$, where $e(j)_{i\alpha}^2$ is the polarization vector for mode j, particle i, direction α (x or y). Essentially, $\langle\omega_{i\alpha}\rangle$ measures the average frequency in which particle i participates in direction α. $\langle\omega_{i\alpha}\rangle$ has a strong correlation with K_{ii} (Fig. 6). Further, the best power-law fit is $\langle\omega_{i\alpha}\rangle \propto K_{ii}^{0.47(1)}$, reminiscent of a simple harmonic oscillator, for which $\omega \propto \sqrt{K}$.

Surprisingly, we find that the location of a particle to have little effect on $\langle\omega_{i\alpha}\rangle$, i.e., $\langle\omega_{i\alpha}\rangle$ is not qualitatively different for particles on the cluster surface as compared to particles in the cluster interior. In either case, $\langle\omega_{i\alpha}\rangle$ simply depends on K_{ii}.

IV. DISCUSSION AND SUMMARY

We have found that the median vibrational frequency, ω_{Med}, of a disordered cluster is predominantly set by $\overline{K_{ii}}$, the ensemble-averaged confining stiffness for particles in the cluster. $\overline{K_{ii}}$, in turn, has a strong correlation with $\overline{NN}$, the average number of nearest neighbors; this latter effect produces the previously observed[3] correlations between $\overline{NN}$ and ω_{Med}. Thus, the present observations suggest that the fundamental origin between $\overline{NN}$ and ω_{Med} is a result of mean confining stiffness in the cluster. Further, the average frequency of an individual particle, $\langle\omega_{i\alpha}\rangle$, increases as a power-law with K_{ii}, i.e., $\langle\omega_{i\alpha}\rangle_i \propto K_{ii}^{0.47(1)}$, a relationship reminiscent of a simple harmonic oscillator. Thus, while the total vibrational spectrum is set by the collective nature of the disordered network, the average vibrations of individual particles are determined primarily by local stiffness.

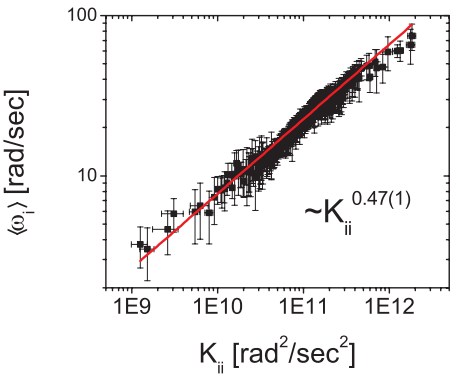

FIG. 6. The eigenvector-weighted frequency, $\langle\omega_{i\alpha}\rangle$, plotted versus diagonal stiffness matrix elements, K_{ii}. Solid red line is the best power-law fit. The relationship between $\langle\omega_{i\alpha}\rangle$ and K_{ii} is reminiscent of a simple harmonic oscillator.

While these results explain properties of disordered clusters, it's natural to consider how they inform other commonly studied systems. Specifically, since the average number of nearest neighbors and mean confining stiffness correlate strongly with the median phonon frequency, our observations suggest that anytime the average number of nearest neighbors is increased in a disordered system, it is likely that the median frequency of the ensemble will increase as well. This effect should apply to different physical systems ranging from athermal jammed packings of purely repulsive particles[4,5] to aging glasses,[15] and the observation suggests a spectroscopic means to probe average coordination and changes thereof.

Finally, the results presented here suggest that the vibrational modes can be shifted to lower (higher) energy by "doping" a glass with particles that are softer (stiffer) than average; these particles would also have especially low (high) average frequencies. This could be accomplished in colloids by mixing hard and soft particles, or by mixing particles with different amounts of surface charge. For atomic or molecular glass-formers, this could be accomplished by mixing so-called "fragile" glasses with "strong" glasses.[20] Interestingly, recent works have suggested that particles in glasses that participate more than average in quasi-localized low frequency modes are more prone to rearrangement.[21–24] Based on our findings, we speculate that regions containing soft "dopant" particles may be likely to rearrange. Alternatively, doping a glass with a small number of especially hard particles could potentially create regions that are unlikely to rearrange. This could potentially also be accomplished by creating regions

with small *NN*, perhaps with laser tweezers, as previous studies found such regions to be associated with enhanced participation in quasi-localized modes.[25,26]

ACKNOWLEDGMENTS

We thank Kevin Aptowicz, Piotr Habdas, Carl Goodrich, and Andrea Liu for helpful discussions, and we gratefully acknowledge financial support from the National Science Foundation through Grant Nos. DMR12-05463, the PENN MRSEC DMR11-20901, and NASA NNX08AO0G. Z.Z. gratefully acknowledges financial support from the National Basic Research Program of China through Grant No. 2012CB821500.

APPENDIX: DERIVATION OF RELATIONSHIP BETWEEN ω_{Med} AND $\overline{K_{ii}}$

The strong relationship between $\overline{K}_{ii}$ and ω_{Med} can be understood from some simple linear algebra. The eigenvalues of the stiffness matrix are obtained from the relation $(K_{ij} - \omega^2 I_{ij})e_{\omega_l} = 0$, where e_{ω_l} is the eigenvector for the lth mode with frequency ω_l and I_{ij} is the identity matrix. If we define a new matrix, $A_{ij} = K_{ij} - cI_{ij}$, where c is a chosen scalar, we can then write $(K_{ij} - \omega_l^2 I_{ij})e_{\omega_l} = (A_{ij} + cI_{ij} - \omega_l^2 I_{ij})e_{\omega_l} = (A_{ij} - [\omega_l^2 - c]I_{ij})e_{\omega_l} = (A_{ij} - \lambda_l I_{ij})e_{\omega_l}$, where λ_l is the lth eigenvalue of A_{ij} (just as ω_l^2 is the lth eigenvalue of K_{ij}. Thus, $\lambda_l = \omega_l^2 - c$ and $\omega_l = \sqrt{\lambda_l + c}$. Note that while ω_l must be positive, λ_l may be positive or negative, depending on the chosen value of c. However, what value should be selected for c?

The median of ω is the Nth mode (there are $2N$ degrees of freedom), ω_N, and $\omega_N = \sqrt{\lambda_N + c}$. If c is chosen such that $c \approx \omega_N^2$, then λ_N is small and ω_N only depends strongly on c. For example, if we set $c = \omega_N^2$, then $\omega_N = \sqrt{\lambda_N + c} = \sqrt{\lambda_N + \omega_N^2}$, so λ_N trivially is 0.

In an attempt to identify an interesting or useful value for c, we next set $c = \overline{K}_{ii}$. We have already seen that $\overline{K}_{ii}$ correlates with ω_{Med}, making it a natural choice. Further, the best linear fit between $\sqrt{\overline{K}_{ii}}$ and ω_{Med} has a slope of nearly 1 (1.09(4)), implying that λ_N is likely small compared to $\sqrt{\overline{K}_{ii}}$. Placing $c = \overline{K}_{ii}$ into the formula above gives us $\omega_{Med} = \sqrt{\lambda_{Med} + \overline{K}_{ii}}$. λ_{Med} can be calculated from the matrix $A_{ij} = K_{ij} - \overline{K}_{ii} I_{ij}$ (Fig. 7). There is little correlation between $\overline{NN}$ and λ, and λ is smaller in magnitude than ω_{Med}^2 (Fig. 7). This relationship should also be expected as Fig. 5 shows that $\overline{K}_{ii}$ is typically larger than ω_{Med}^2, which, in turn, requires that λ is negative.

While we have experimentally demonstrated that λ_{Med} is small compared to $\overline{K}_{ii}$, could we have predicted this relationship based on the overall shape of K_{ij}? If A_{ij} were a random matrix, its median eigenvalue would be 0, according to the Wigner semi-circle law.[27] Of course, A_{ij} is not a truly random matrix. Thus, further study is required to elucidate the origin of the relationship between $\overline{K}_{ii}$ and ω_{Med}.

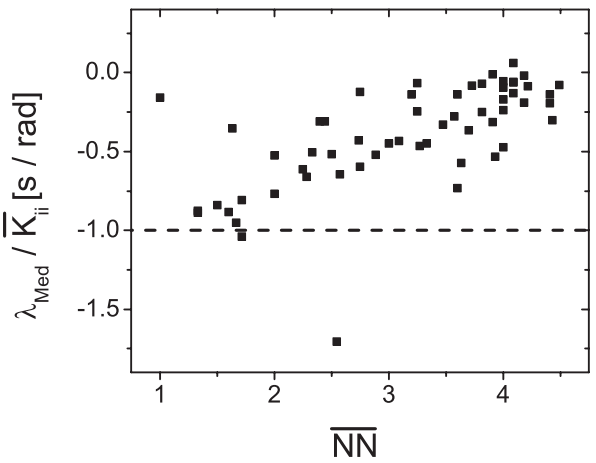

FIG. 7. The eigenvalues, λ, of matrix $A_{ij} = K_{ij} - \overline{K}_{ii} I_{ij}$, normalized by the mean of the diagonal value of the stiffness matrix, i.e., $\overline{K}_{ii}$, and plotted versus the number of neighbors *NN*.

[1] G. Meng, N. Arkus, M. P. Brenner, and V. N. Manoharan, Science **327**, 560 (2010).
[2] P. J. Lu, J. C. Conrad, H. M. Wyss, A. B. Schofield, and D. A. Weitz, Phys. Rev. Lett. **96**, 028306 (2006).
[3] P. J. Yunker, K. Chen, Z. Zhang, and A. G. Yodh, Phys. Rev. Lett. **106**, 225503 (2011).
[4] C. S. O'Hern, S. A. Langer, A. J. Liu, and S. R. Nagel, Phys. Rev. Lett. **88**, 075507 (2002).
[5] M. Wyart, S. R. Nagel, and T. A. Witten, EPL **72**, 486 (2005).
[6] Z. Zhang, P. J. Yunker, P. Habdas, and A. G. Yodh, Phys. Rev. Lett. **107**, 208303 (2011).
[7] D. Beysens and T. Narayanan, J Stat. Phys. **95**, 997 (1999).
[8] C. Hertlein, L. Helden, A. Gambassi, S. Dietrich, and C. Bechinger, Nature (London) **451**, 172 (2008).
[9] F. Soyka, O. Zvyagolskaya, C. Hertlein, L. Helden, and C. Bechinger, Phys. Rev. Lett. **101**, 208301 (2008).
[10] A. Ghosh, R. Mari, V. Chikkadi, P. Schall, J. Kurchan, and D. Bonn, Soft Matter **6**, 3082 (2010).
[11] K. Chen, W. G. Ellenbroek, Z. Zhang, D. T. N. Chen, P. J. Yunker, S. Henkes, C. Brito, O. Dauchot, W. van Saarloos, and A. J. Liu *et al.*, Phys. Rev. Lett. **105**, 025501 (2010).
[12] D. Kaya, N. L. Green, C. E. Maloney, and M. F. Islam, Science **329**, 656 (2010).
[13] A. Ghosh, V. K. Chikkadi, P. Schall, J. Kurchan, and D. Bonn, Phys. Rev. Lett. **104**, 248305 (2010).
[14] Z. Zhang, N. Xu, D. T. Chen, P. Yunker, A. M. Alsayed, K. B. Aptowicz, P. Habdas, A. J. Liu, S. R. Nagel, and A. G. Yodh, Nature (London) **459**, 230 (2009).
[15] P. Yunker, Z. Zhang, K. B. Aptowicz, and A. G. Yodh, Phys. Rev. Lett. **103**, 115701 (2009).
[16] P. Yunker, Z. Zhang, and A. G. Yodh, Phys. Rev. Lett. **104**, 015701 (2010).
[17] D. G. Grier, Nature (London) **424**, 810 (2003).
[18] C. Brito and M. Wyart, EPL **76**, 149 (2006).
[19] K. Chen, T. Still, K. B. Aptowicz, S. Schoenholz, M. Schindler, A. C. Maggs, A. J. Liu, T. Lubensky, and A. G. Yodh, "Phonons in pristine and imperfect two-dimensional soft colloidal crystals," arXiv:1212.1741.
[20] C. A. Angell, Science **267**, 1924 (1995).
[21] M. L. Manning and A. J. Liu, Phys. Rev. Lett. **107**, 108302 (2011).
[22] K. Chen, M. L. Manning, P. J. Yunker, W. G. Ellenbroek, Z. Zhang, A. J. Liu, and A. G. Yodh, Phys. Rev. Lett. **107**, 108301 (2011).
[23] A. Widmer-Cooper, H. Perry, P. Harrowell, and D. R. Reichman, Nat. Phys. **4**, 711 (2008).
[24] A. Ghosh, V. Chikkadi, P. Schall, and D. Bonn, Phys. Rev. Lett. **107**, 188303 (2011).
[25] H. Shintani and H. Tanaka, Nat. Mater. **7**, 870 (2008).
[26] P. Tan, N. Xu, A. B. Schofield, and L. Xu, Phys. Rev. Lett. **108**, 095501 (2012).
[27] E. P. Wigner, Ann. Math. **67**, 325 (1958).